Integrated Ferroelectrics, 111: 27–36, 2009
Copyright © Taylor & Francis Group, LLC
ISSN 1058-4587 print / 1607-8489 online
DOI: 10.1080/10584580903586646

The Optical Dielectric Function in Monolithic $Ba_xSr_{1-x}TiO_3$ Films

D. Bruzzese,[1] K. J. Fahnestock,[1] C. L. Schauer,[1] J. E. Spanier,[1,*] C. V. Weiss,[2] S. P. Alpay,[2] M. W. Cole,[3] N. M. Sbrockey,[4] and G. S. Tompa[4]

[1]Department of Materials Science and Engineering, Drexel University, PA 19104
[2]Materials Science and Engineering Program, Department of Chemical, Materials, and Biomolecular Engineering, University of Connecticut, CT 06269
[3]U. S. Army Research Laboratory, Aberdeen Proving Grounds, MD 20783
[4]Structured Materials Industries, Inc., 201 Circle Drive North, Unit #102, Piscataway, NJ 08854

Downloaded By: [University of Connecticut] At: 16:44 15 September 2010

ABSTRACT

We present the results of characterization and analysis of the optical dielectric function of monolithic $Ba_xSr_{1-x}TiO_3$ films prepared by metal-organic solution deposition (MOSD). Lorentz Oscillator + Drude parameters and band gap for selected compositions are determined from variable-angle spectroscopic ellipsometry. Variation of the complex optical dielectric function is seen, and the results suggest that spectroscopic ellipsometry can be an effective means of both *ex situ* analysis and *in situ* monitoring of film composition during other BST and related film material growth processes.

Keywords: Ferroelectric thin films, phase shifters, BST, spectroscopic ellipsometry, optical dielectric function

INTRODUCTION

Thin-film barium strontium titanate, $Ba_xSr_{1-x}TiO_3$ (BST) is a complex oxide consisting of a solid solution of ferroelectric barium titanate $BaTiO_3$ (BTO) and the (quantum) paraelectric strontium titanate $SrTiO_3$ (STO). BST continues to attract significant interest due to its applicability as a high frequency low loss tunable dielectric material. Variation of the BST stoichiometry and ferroelectric polarization along the vertical axis toward pure BTO (e.g. graded multilayers)

Received August 16, 2009; in final form December 16, 2009.
*Corresponding author. E-mail: spanier@drexel.edu

has been shown to provide a dielectric function temperature insensitivity, [1] along with an increased dielectric response and low dielectric loss relative to the monolithic (pure BTO) case. Such designs increase device performance and utility in a number of applications, including as a tunable microwave communication technology. For BST to become more widely adopted and integrated, it must be produced by a scalable process such as metallorganic chemical vapor deposition (MOCVD). [2, 3] Growth of complex oxide films in monolithic and graded form for these and related applications demands methods for rapid *ex situ* analysis of film composition and uniformity, and *in situ* characterization of composition during growth.

Tcheliebou et al. [4] presented a study of the optical dielectric function in monolithic films of BST grown by pulsed laser deposition (PLD) on $(1\bar{1}02)$ sapphire over the range 382–800 nm from transmission measurements using an abbreviated Cauchy model and an individual dipole oscillator model. RF magnetron sputtering of BST on p-type silicon and glass were studied by B. Panda et al. [5] with transmittance and ellipsometry to investigate the dispersion and band gap dependence on composition. This was also independently confirmed as reported in Refs. 4 and 5. More recently, Zelenzy [11] studied PLD-produced $Ba_{0.75}Sr_{0.25}TiO_3$ (75/25) on platinized silicon by a combination of reflectance and ellipsometry using a Cauchy model in the transparent wavelength range and the Cody-Lorentz model around and below the absorption edge.

The main goal of this work is to demonstrate that successful analysis of variable-angle spectroscopic ellipsometry data collected from monolithic BST films can be used to investigate and quantify the BST thin film composition, thickness d, and interfacial abruptness. Here we present a characterization of the optical properties of several metallorganic solution-deposited (MOSD) films of different composition and values of thickness. Here, MOSD is a process whereby different metallic precursors are separately dissolved and then combined in solution in an appropriate stoichiometric ratio, then spin coated onto a silicon or platinized silicon substrate, pyrolized, and finally annealed. MOSD has enabled rapid study and optimization of monolithic and graded thin film materials for device applications.

Variable-temperature dielectric characterization, topographic atomic force microscopy (AFM), and scanning electron microscopy (SEM) of the MOSD films were performed to characterize the dielectric response, surface roughness and general microstructure; dielectric measurement results will be reported elsewhere. The films are polycrystalline and perovskite phase as confirmed by x-ray diffraction (XRD), and the composition of the films was verified by Rutherford backscattering spectroscopy and Auger electron spectroscopy as reported elsewhere. [7, 8] The spectroscopic ellipsometry data were fitted by carrying out a constrained optimization of fitting parameters for several selected trial dielectric function models, including known interfacial and surface layers. A global modified Levenberg-Marquart algorithm was used to minimize

Downloaded By: [University of Connecticut] At: 16:44 15 September 2010

the total root-mean squared error (RMSE) values. In particular, the Lorentz oscillator model, including an additional Drude term, was chosen because of its appropriateness within the spectral region of the optical bandgap.

Spectroscopic ellipsometry [9, 10] is a versatile analytical method which measures the change in polarization upon reflection of incident linearly polarized light from one or more films on a semi-infinite substrate; it is routinely carried out as a function of wavelength and angle of incidence. Measured is the ratio of parallel-to-perpendicularly polarized light by use of a rotating analyzer, and is expressed by the ellipsometric parameters ψ and Δ, $\rho = \frac{\tilde{R}_P}{\tilde{R}_S} = \tan(\psi)e^{i\Delta}$ where ψ is the change in amplitude and Δ is the change in phase of the reflected light. The complex Fresnel reflection coefficients $\tilde{R}_s$ and $\tilde{R}_p$ are related to the index of refraction and extinction coefficient of each layer in the system by Snell's law.

Two different dispersion function models were considered. Although the Cauchy model $n(\lambda) = A_n + \frac{B_n}{\lambda^2} + \frac{C_n}{\lambda^4}$ and $k(\lambda) = A_k + \frac{B_k}{\lambda^2} + \frac{C_k}{\lambda^4}$ is purely phenomenological and is without physical basis, its application results in a reasonable description of the shape of the dispersion curve below the bandgap. A more physically relevant model, the Lorentz Oscillator + Drude (LOD), assumes a number of oscillators which resonate at one or more frequencies, and includes the effect of free-carriers as well as lattice dispersion, though this contribution may be negligible. The Drude component in the function accounts for delocalized electrons, and it is more applicable for metallic systems. However, if the material is non-metallic and does not possess free electrons, then its contribution to the dielectric function is negligible, and thus its inclusion does not detract from the accuracy of the model. The number of oscillators is system-specific, but from initial modeling and Refs. 4 and 5, a single oscillator is suggested. The form of the single oscillator LOD is $\tilde{\varepsilon}(E) = \varepsilon_\infty(1 + \frac{A^2}{E_C^2 - E(E - iv)} - \frac{\omega_p^2}{E(E + i\Gamma)})$ where ε_∞ is the high frequency lattice dielectric constant, ω_p is the plasma frequency, Γ the collision frequency, E_C is the center energy of the oscillator, A is the strength of the oscillator and v is the vibrational frequency of the oscillator.

Downloaded By: [University of Connecticut] At: 16:44 15 September 2010

EXPERIMENTAL: Surface Characterization and Reflectance & Ellipsometry

Surface Characterization

Several samples were prepared for this study by the MOSD method. Films were prepared on silicon with a native oxide layer as well as on platinized silicon. Barium acetate and strontium acetate were the precursors used in the synthesis of the films. (A complete description of synthesis is presented in Refs. 7 and 8.) Cross-sections of the monolithic BST samples were prepared and viewed by field emission SEM (Amray 1850 FE-SEM) to provide an

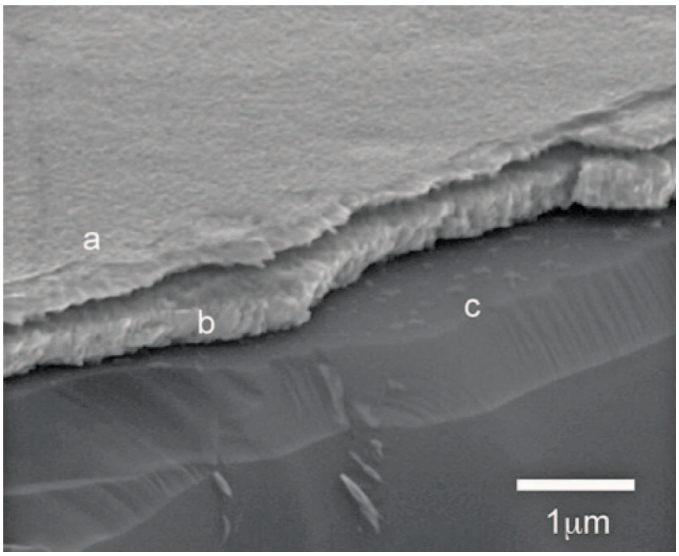

Figure 1. Scanning electron micrograph (SEM) of an MOSD-produced monolithic BST film deposited on a platinized SiO_2/Si substrate. In the figure, a denotes the BST film, b the Pt layer, and c the SiO_2/Si substrate.

Downloaded By: [University of Connecticut] At: 16:44 15 September 2010

estimate of thickness and to verify the accuracy of the model (Fig. 1). Surface roughness was obtained using AFM (Asylum Research MFP3D, Santa Barbara, CA). Scans were performed over a 25 μm^2 area and showed RMS roughness values of 9–17 nm depending on sample thickness. Reflectivity measurements were performed using a Shimadzu UV-2501PC UV-VIS spectrophotometer in the range 250 nm–1000 nm. Spectroscopic ellipsometry was performed (J.A. Woollam, Model M-2000U, Lincoln, NE) from 245–1000 nm and at angles of 60°, 65°, 70°, and 75° from normal, and analysis was aided by the WVASE32 and Film Wizard (SCI, San Diego CA) software packages. Analysis of the data showed that data acquired at 70° and 75° exhibited the least depolarization, and these data were used in modeling.

Values for surface roughness δ obtained by AFM were used as an input in the thin film modeling and analysis. A single value for roughness was the starting point for the model, depending on deposition technique and substrate used. The typical values of roughness for different substrates are shown in Table 1.

Reflectance and Ellipsometry

Shown in Figs. 2a and b are the variations in Ψ and Δ for different thicknesses of the same composition, and different compositions at roughly the same

Table 1
Typical roughness values for various compositions of monolithic BST on Pt.

Substrate	Ba/Sr Ratio	RMS (nm)	Scan area
Pt on Si	70/30	16.56	5 μm × 5 μm
Pt on Si	80/20	11.42	5 μm × 5 μm
Pt on Si	90/10	8.87	5 μm × 5 μm

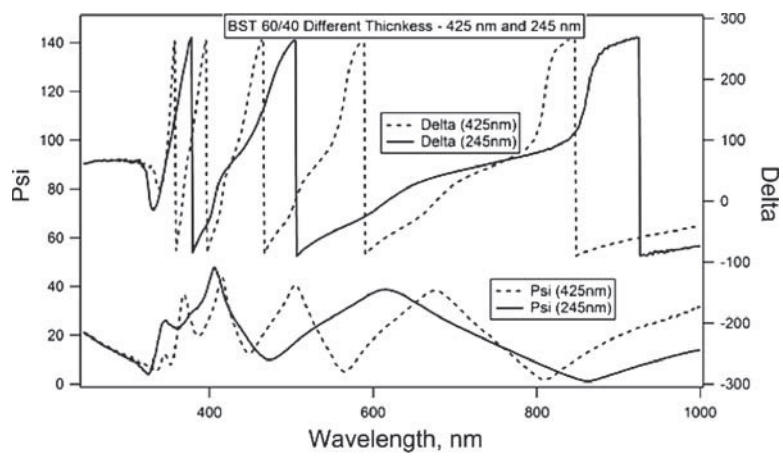

(a)

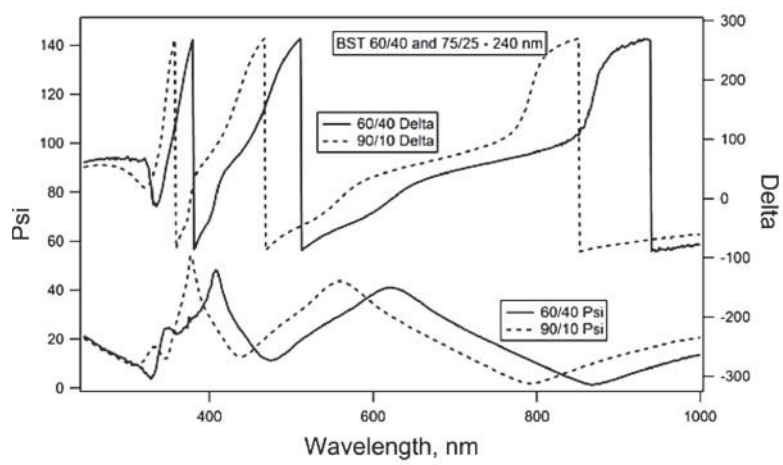

(b)

Figure 2. Ψ (left axis) and Δ (right axis) for two samples of the same composition but different thicknesses (a) and for two samples of the same thickness but different composition (b).

Downloaded By: [University of Connecticut] At: 16:44 15 September 2010

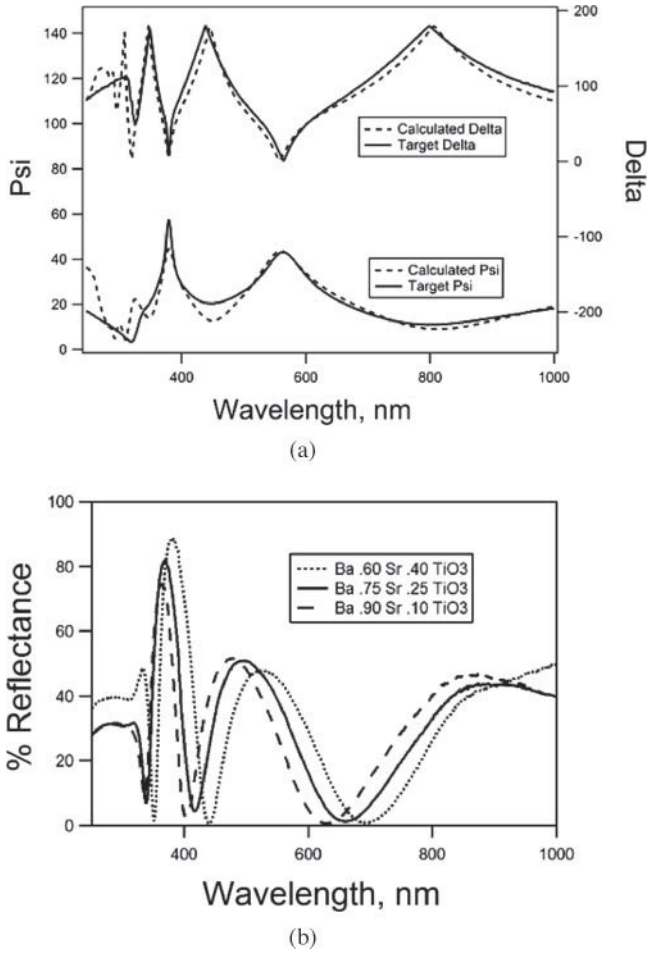

Figure 3. a,b-Representative model fitting results for calculated Ψ and Δ (top) as compared with experimental data. Reflectance data (bottom) for three different compositions is shown.

thickness, demonstrating the variations in ellipsometric parameters are independent of with thickness and composition. Shown in Fig. 3a are the experimentally obtained Ψ and Δ and the calculated functions Ψ and Δ which result after optimization of the free parameters in the model; measured reflectance is displayed in Fig. 3b. The appearance of interference fringes indicate that the roughness of the film is well within a fraction of a wavelength, and that the thickness is on the order of an optical wavelength.

Downloaded By: [University of Connecticut] At: 16:44 15 September 2010

RESULTS AND DISCUSSION

Initial guesses for dispersion with the LOD model were obtained by performing a linear interpolation of tabular data for the index of refraction and extinction coefficient from pure BTO to pure STO from Palik. [5] These data are then converted into LOD parameters and serve as the initial guesses for the model. Because the wavelength of the bandgap λ_g of BST is 345 nm $< \lambda_g <$ 360 nm [4, 5] our modeling using the Cauchy distribution function can only be performed in the range 400 nm $\leq \lambda \leq$ 1000 nm. To observe the bandgap one cannot use an unmodified Cauchy function; instead we applied the LOD model here. Others have reported on the dependence of index of refraction with composition as well as that of bandgap on composition. [4, 5] Consistent with previously reported work, we find that experimental evaluation of band gap in these complex oxide perovskite solid solutions is a good indicator of composition as it varies consistently with composition.

LOD modeling was performed in the spectral range 300 nm $\leq \lambda \leq$ 1000 nm. Shown in Fig. 4 (left) are the calculated optical dispersions. We used a geometry which consisted of a surface roughness layer represented by a Bruggeman effective medium approximation. The representative model geometry is pictured in the inset of Fig. 4 (left). The six LOD fitting parameters were allowed to vary, along with the thicknesses of the surface roughness and BST layer. The results are listed in Tables 2 and 3. RMSE values were typically around 6, and this relatively large value is likely due to the large number of fitting parameters;

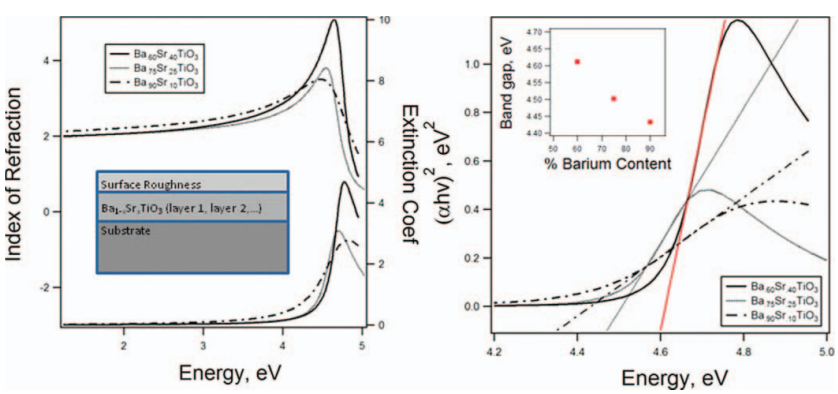

Figure 4. (left) Modeled dispersion of three different compositions of BST with model geometry in inset. (right) extrapolation of absorption plot to infer band gap, which is plotted in the inset, shown as a function of barium content. (See Color Plate VI)

Downloaded By: [University of Connecticut] At: 16:44 15 September 2010

Table 2
Lorentz+Drude parameters of films of different composition and thickness.

Composition Substrate	60/40 SiO_2/Si	70/30 Pt/SiO_2/Si	75/25 SiO_2/Si	80/20 Pt/SiO_2/Si	90/10(A) SiO_2/Si	90/10(B) Pt/SiO_2/Si
ε_∞	6.82	1.84	3.09	2.84	2.43	2.65
ω_p	1.00	0.94	0.41	0.30	0.36	0.34
Γ	0.99	9.99	0.17	8.32	0.32	0.12
A	9.27	4.49	2.70	3.16	3.40	3.96
E_C	5.29	4.83	4.63	4.53	4.71	4.69
v	0.16	0.35	0.27	0.24	0.23	0.59
d, nm	433	579	228	500	234	487
δ, *nm*	6.8	10.7	1.7	7.2	4.8	4.3
RMSE	7.28	13.8	7.35	5.57	7.15	4.81

subsequent analysis will reduce the number of free parameters through parallel investigation of the parameters by other methods.

We have analyzed the bandgap by modeling the extinction coefficient with the LOD model. To obtain the composition-dependence of the bandgap E_g, we calculated the absorption coefficient α as a function of λ via $\alpha = \frac{4\pi k}{\lambda}$ and we extrapolated the linear portion of a plot of $(\alpha h v)^2$ vs. energy to its intersection with the energy axis, as shown in Fig. 4b. Here, we have assumed a direct gap, namely $\alpha h v = K \times (v - E_g)^{1/r}$ where $r = 2$ and K is a constant. The obtained values (see inset of Fig. 4b) are comparable to those reported from BST produced using sol-gel processing [11].

Table 3
Lorentz+Drude parameters of six different films of identical composition.

Composition Substrate	60/40_1 SiO_2/Si	60/40_1b SiO_2/Si	60/40_2 SiO_2/Si	60/40_3 SiO_2/Si	60/40_4 SiO_2/Si	60/40_5 SiO_2/Si	60/40_6 SiO_2/Si
ε_∞	1.05	1.25	1.00	2.24	2.12	2.68	2.13
ω_p	1.99	4.25	0.99	0.24	0.54	0.54	1.8
Γ	0.02	497.63	19.77	0.89	12.82	0.05	165.71
A	8.14	7.04	9.27	4.16	4.44	3.69	4.24
E_C	4.46	4.99	5.29	4.74	4.74	4.77	4.72
v	0.08	0.19	0.16	0.22	0.15	.18	0.22
d, nm	279	250	433	240	398	267	244
δ, *nm*	9.89	5.4	6.8	4.7	6.6	4.4	5.6
RMSE	9.31	6.75	7.28	7.32	7.83	6.56	7.60

Downloaded By: [University of Connecticut] At: 16:44 15 September 2010

CONCLUSIONS

A characterization of the optical dielectric function of $Ba_xSr_{1-x}TiO_3$ of selected composition and thickness was performed. We have applied the LOD model to our analysis of the data to obtain parameters for the dispersion of the material, and then to obtain the composition-dependent band gap. We found a correlation between composition and bandgap in the results obtained for MOSD-produced films. Though further work is needed, particularly involving the application of spectroscopic ellipsometry to the evaluation of the optical properties of compositionally modulated BST, this work suggests that *in situ* analysis of composition during growth may be possible. Ongoing work includes analysis of applicability of other models to this system and improvement of its accuracy, and applying the model to evaluating interfacial sharpness in more detail.

Downloaded By: [University of Connecticut] At: 16:44 15 September 2010

ACKNOWLEDGMENTS

This work was supported by the Army Research Office under W911NF-08-C-0124 and W911NF-08-1-0067. C.L.S acknowledges support from the NSF under CMMI-0804543.

REFERENCES

1. Z. Cao, A. Ding, X. He, W. Cheng, and P. Qiu, *J. Cryst. Growth* **270**, 168 (2004).
2. M. W. Cole, P. C. Joshi, and M. Ervin, *J. Appl. Phys.* **89**, 6336 (2001).
3. M. W. Cole, P. C. Joshi, M. Ervin, M. Wood, and R. L. Pfeffer, *Thin Solid Films* **374**, 34 (2000).
4. F. Fitsilis, S. Regnery, P. Ehrhart, R. Waser, F. Schienle, M. Schumacher, M. Dauelsberg, P. Strzyzewski, and H. Juergensen, *J. Euro. Ceram. Soc.* **21**, 1547 (2001).
5. E. Palik and G. Ghosh, *Handbook of Optical Constants of Solids*. San Diego: Academic Press; 1985.
6. H. Tian, W. Luo, A. Ding, J. Choi, C. Lee, and K. No, *Thin Solid Films* **408**, 200 (2002).
7. M. W. Cole, E. Ngo, S. Hirsch, J. D. Demaree, S. Zhong, and S. P. Alpay, *J. Appl. Phys.* **102**, 34104 (2007).
8. P. Ehrhart, F. Fitsilis, S. Regnery, R. Waser, F. Schienle, M. Schumacher, H. Juergensen, and W. Krumpen, *Integr. Ferroelectr.* **45**, 59 (2002).

9. B. Panda, A. Dhar, G. D. Nigam, D. Bhattacharya, and S. K. Ray, *Thin Solid Films* **332**, 46 (1998).
10. F. Tcheliebou, H. S. Ryu, C. K. Hong, W. S. Park, and S. Baik, *Thin Solid Films* **299**, 14 (1997).
11. V. Železný, D. Chvostová, L. Pajasová, M. Jelínek, T. Kocourek, S. Danis, and V. Valvoda, *Appl. Surf. Sci.* **255**, 5280 (2009).

Downloaded By: [University of Connecticut] At: 16:44 15 September 2010